Electrochimica Acta 97 (2013) 210–215

Contents lists available at SciVerse ScienceDirect

Electrochimica Acta

journal homepage: www.elsevier.com/locate/electacta

Superior charge-transfer kinetics of NASICON-type $Li_3V_2(PO_4)_3$ cathodes by multivalent Al^{3+} and Cl^- substitutions

J.N. Son [a], S.H. Kim [a], M.C. Kim [a], G.J. Kim [a], V. Aravindan [a,b], Y.G. Lee [c], Y.S. Lee [a,*]

[a] Faculty of Applied Chemical Engineering, Chonnam National University, Gwang-ju 500-757, Republic of Korea
[b] Energy Research Institute @ NTU (ERI@N), Nanyang Technological University, Singapore 637553, Singapore
[c] Power Control Device Research Team, Electronics and Telecommunications Research Institute, Daejeon 305-700, Republic of Korea

ARTICLE INFO

Article history:
Received 19 January 2013
Received in revised form 24 February 2013
Accepted 24 February 2013
Available online 1 March 2013

Keywords:
Li-ion batteries
NASICON-type $Li_3V_2(PO_4)_3$
Anion doping
Carbon coating

ABSTRACT

The kinetic properties of Li insertion in NASICON-type $Li_3V_2(PO_4)_3$ cathodes were enhanced substantially by Al^{3+} and Cl^- multivalent substitutions of various concentrations. Pristine and carbon coated, Al-doped $Li_3V_2(PO_4)_3$ were also prepared by a conventional solid-state approach under optimized conditions. Samples phase purity was investigated through X-ray diffractometry. Li insertion was studied in half-cells at 3-4.8 V *vs.* Li for the removal of 3 mol of Li. Carbon-coated $Li_3V_{1.98}Al_{0.02}(PO_4)_{2.99}Cl_{0.01}$ showed the highest reversible insertion of 2.71 mol of Li (178 mAh g^{-1}) at a current density of 0.2 mA cm^{-2}. It showed a capacity retention of over 80% after 100 cycles. Cl^- substitution led to improved performance under harsh conditions of 15 C rate and high temperature (50 °C). The enhancement of Li ion kinetics was demonstrated through cyclic voltammetry in a two-electrode configuration and electrochemical impedance spectroscopy confirmed the enhanced conductivity.

1. Introduction

Since the discovery of Li ions reversible insertion and extraction in $LiFePO_4$ polyanionic frameworks [1] much work has sought to develop high-performance, Li-ion cells containing $(PO)_4^{3-}$ based electrodes [2–4]. $(PO)_4^{3-}$ can increase thermal stability because strong P—O bonds are present in both the lithiated and the delithiated states and inductive effects of such anion lead to very flat charge–discharge profiles [2,5–7]. Several polyanionic frameworks, such as $LiMnPO_4$, $LiCoPO_4$, $Li_3V_2(PO_4)_3$, and $LiTi_2(PO_4)_3$, have been explored as possible electrodes for Li-ion batteries (LIB) [2,7–11]. Similarly, $(PO)_4^{3-}$ based fluorophosphates have also been investigated as prospective electrodes for LIBs for example $LiVPO_4F$ [12], $Li_5V(PO_4)_2F_2$ [13], $LiFePO_4F$ [14], $LiTiPO_4F$ [15], Li_2CoPO_4F [16], Li_2MnPO_4F [17] Li_2FePO_4F and Na_2FePO_4F [18].

$Li_3V_2(PO_4)_3$ is a promising cathode material for lithium battery. It shows a high theoretical capacity of ~197 mAh g^{-1} for the removal of 3 mol of lithium and high thermal and electrochemical stabilities. It is simple and inexpensive to prepare and can operate at high potentials [7]. However, distorted arrangements of VO_6 octahedral units in the NASICON structure provide inherent conducting properties. To overcome this issue carbon coating and doping at vanadium sites are attempted and improvement in the electrochemical properties of $Li_3V_2(PO_4)_3$ have resulted [6]. The removal of the third Li ion in monoclinic $Li_3V_2(PO_4)_3$ destroys the structure, leading to severe capacity fading during charging and discharging. Therefore, most research has been limited to the removal of only 2 mol of lithium (theoretical capacity ~132 mAh g^{-1}) from the matrix to allow stable cycling [13]. Monoclinic $Li_3V_2(PO_4)_3$ can exhibit good electrochemical properties through carbon coating or vanadium site doping; though the removal of 2 or 3 mol of Li is kinetically slow, which makes achieving the theoretical capacity difficult. Improved Li-ion kinetics is necessary to achieve high-performance electrodes in practical cells.

Irrespective of the structure, $(PO)_4^{3-}$ based materials generally exhibit poor conductivity and hence less work has attempted to increase inherent conductivity by modifying anion sites. Kang and Ceder [19] demonstrated that oxygen-deficient, olivine-phase $LiFePO_4$ ($LiFe_{0.9}P_{0.95}O_{4-\delta}$) showed ultrafast charge–discharge capabilities and improved Li insertion kinetics. Lee et al. [20] reported sulfur-substituted, olivine-phase $LiFePO_4$ ($LiFePO_{3.98}S_{0.03}$) with enhanced performance at high temperatures of 50 and 60 °C. Pan et al. [21] reported fluorine-substituted, carbon-coated, olivine phosphate (C-$LiFe(PO_4)_{0.85}F_{0.15}$) with improved high-current and kinetic properties. Goodenough and co-workers [22] reported the improved charge-transfer kinetics of $LiFePO_4$ by anion site modifications with sulfur and nitrogen *via* density functional theory (DFT) calculations. Zhong et al. [23] demonstrated that the fluorine doping of oxygen sites in $Li_3V_2(PO_4)_3$ material ($Li_3V_2(PO_4)_{2.9}F_{0.1}$) improved Li insertion properties.

* Corresponding author. Tel.: +82 62 530 1904; fax: +82 62 530 1909.
E-mail addresses: aravind.van@yahoo.com (V. Aravindan), leeys@chonnam.ac.kr (Y.S. Lee).

0013-4686/$ – see front matter © 2013 Elsevier Ltd. All rights reserved.
http://dx.doi.org/10.1016/j.electacta.2013.02.118

Chlorine doping can also improve the electronic properties of $LiFePO_4$ by perfectly replacing oxygen in the tetraheldral sites [24]. This has been confirmed through DFT calculations by Dinh et al. [25]. Sun et al. [26] demonstrated C-$LiFePO_4$ cathodes with improved electrochemical properties and improved Li insertion kinetics under harsh conditions (20 C) through chlorine doping. Yan et al. [24] produced chlorine doping on anion sites along with carbon coating for $Li_3V_2(PO_4)_3$ and found the improved electrochemical properties for the removal of 2 mol of Li.

The influence of Cl^- substitution in the anion sites of NASICON-type $Li_3V_2(PO_4)_3$ for the removal of 3 mol of Li has not yet been studied. Hence, this work reports the removal of 3 mol of Li by the substitution of Al^{3+} and Cl^- in vanadium and anion sites, respectively, along with carbon coating. Further, this work draws on previous work reporting the optimization of Al^{3+} doping and carbon coating. C-$Li_3V_{1.98}Al_{0.02}(PO_4)_3$ was chosen for Cl^- substitution [9]. It is well known that, vanadium site doping enhances ionic conductivity whereas carbon coating improves the electronic conductivity of NASICON-type $Li_3V_2(PO_4)_3$. Here, the effects of Cl^- concentration on the electrochemical properties of C-$Li_3V_{1.98}Al_{0.02}(PO_4)_{3-x}Cl_x$ (x = 0.01, 0.03 and 0.05) are reported for the first time.

2. Experimental

Al^{3+} and Cl^- substituted NASICON-type $Li_3V_2(PO_4)_3$ materials were prepared by a solid-state approach. All chemicals were of analytical grade and used without further purification. Briefly, stoichiometric amounts of Li_2CO_3 (Wako, Japan), V_2O_5 (Sigma–Aldrich, USA), $Al(OH)_3$ (Sigma–Aldrich, USA), $(NH_4)_2HPO_4$ (Sigma–Aldrich, USA) and adipic acid (Sigma–Aldrich, USA) were finely ground in an agate mortar and calcined at 300 °C for 4 h to eliminate ammonium and hydroxyl moieties. Then the intermediate product was thoroughly ground and formed into a pellet, which was sintered at 900 °C for 8 h under an Ar flow to yield single-phase, carbon-coated $Li_3V_{1.98}Al_{0.02}(PO_4)_3$ (hereafter abbreviated as C-$Li_3V_{1.98}Al_{0.02}(PO_4)_3$). Chlorine-substituted samples (C-$Li_3V_{1.98}Al_{0.02}(PO_4)_{3-x}Cl_x$, x = 0.01, 0.03 and 0.05) were similarly prepared using appropriate amounts of NH_4Cl (Sigma–Aldrich, USA). Structural properties were analyzed by X-ray diffraction measurements (Rint 1000, Rigaku, Japan) equipped with CuKα radiation. Powders surface morphologies were studied by scanning electron microscopy (FE-SEM, S4700, Hitachi, Japan) and transmission electron microscopy (TEM, TECNAI, Philips, Netherlands). Standard CR2032 coin cells were assembled for the evaluation of the electrochemical properties of the materials. Test electrodes were formulated with 20 mg active material, 3 mg Ketzen black and 3 mg conductive binder (Teflonized acetylene black, TAB-2). They were pressed on a 200 mm^2 area stainless steel mesh, which served as the current collector, and dried at 160 °C for 4 h in a vacuum oven. Coin-cells were assembled in an Ar-filled glove box. Test cells were constructed with composite cathode, metallic lithium anode and porous polypropylene film separator (Celgard 3401, USA) with an electrolyte of 1 M $LiPF_6$ in ethylene carbonate (EC)/dimethyl carbonate (DMC, 1:1 by vol., Techno Semichem Co., Ltd., Korea). Cyclic voltammetry (CV) and electrochemical impedance spectroscopic (EIS) studies were conducted by two-electrode setup using a Bio-Logic electrochemical work station (SP-150, Biologic, France), in which metallic lithium acts as both working and counter electrode. Galvanostatic charge–discharge testing was conducted between 3 and 4.8 V *vs.* Li at a current density of 0.2 mA cm^{-2} at ambient and elevated temperatures.

3. Results and discussion

Fig. 1(a) shows the typical powder X-ray diffraction (XRD) pattern of NASICON type $Li_3V_2(PO_4)_3$ powders. The observed

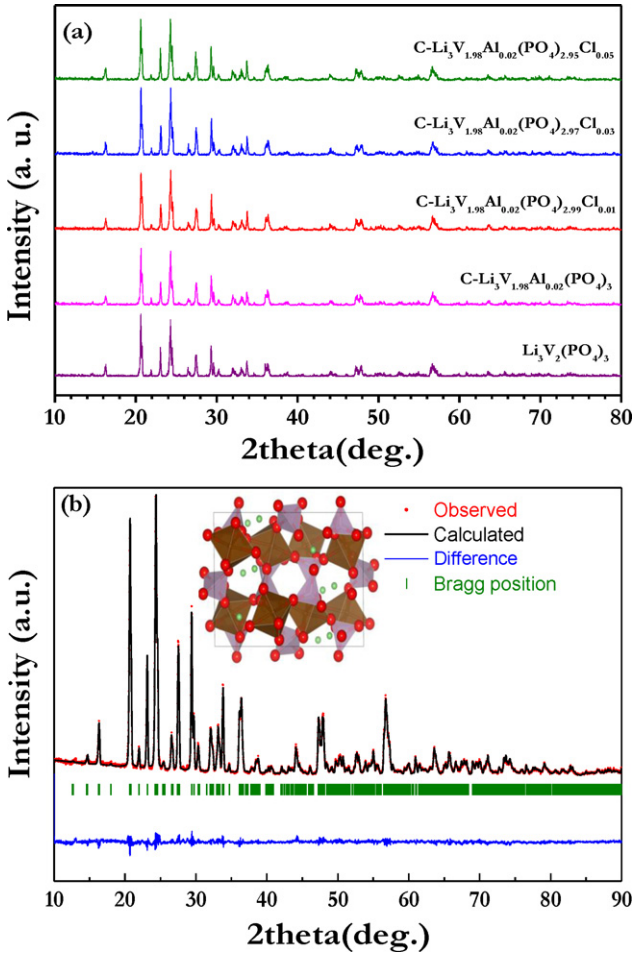

Fig. 1. (a) X-ray diffraction patterns of $Li_3V_2(PO_4)_3$ and C-$Li_3V_{1.98}Al_{0.02}(PO_4)_{3-x}Cl_x$ (x = 0.01, 0.03, and 0.05) materials, and (b) Rietveld analysis result of C-$Li_3V_{1.98}Al_{0.02}(PO_4)_{2.99}Cl_{0.01}$.

XRD reflection clearly indicates the formation of single phase compounds without any impurity traces and it belongs to monoclinic structure with $P2_1/n$ space group [7]. The substitution of Al^{3+} and Cl^- in vanadium and oxygen sites did not affect the formation of a single phase and this is probably due to the concentration of both Al^{3+} and Cl^- is found too low to induce the structural change. The presence of Cl^- ions in the compounds was confirmed though EDAX analysis (Figure S1). Rietveld analysis also showed that the C-$Li_3V_{1.98}Al_{0.02}(PO_4)_{2.99}Cl_{0.01}$ structure comprised three-dimensional frameworks of VO_6 octahedral units and PO_4 tetrahedral units sharing oxygen vertices (Fig. 1(b)). Each VO_6 octahedral unit was surrounded by six PO_4 tetrahedral units; each tetrahedral unit was surrounded by four VO_6 octahedral units [7]. This configuration forms a three-dimensional network and the alkali cation, Li, is located in the cavities within the framework. Three four-fold crystallographic positions exist for the lithium atoms, leading to twelve lithium positions within the unit-cell [27]. Such an arrangement gives inferior conductivity; hence carbon coating was employed along with substitutions at vanadium and oxygen sites. There is no big difference compared with C-$Li_3V_{1.98}Al_{0.02}(PO_4)_3$ material in crystallographic aspect during Cl^- substitution. However, reduction in lattice parameter values describes the Al^{3+} doping and further increase in values corresponds to the substitution of Cl^- in O atom positions which is clearly evident from Table 1 and Figure S2 [22,26].

Half cells were tested to assess cycling during the removal of 3 mol of lithium. Cells were cycled at 3.0-4.8 V *vs.* Li at a constant

Table 1
Lattice parameter values of selected NASICON type compounds.

	$Li_3V_2(PO_4)_3$	C-$Li_3V_{1.98}Al_{0.02}(PO_4)_3$	C-$Li_3V_{1.98}Al_{0.02}(PO_4)_{2.99}Cl_{0.01}$
a (Å)	8.6160	8.59654(8)	8.5996 (8)
b (Å)	8.5947	8.58481(7)	8.5862 (8)
c (Å)	12.0420	12.02725(10)	12.0302 (11)
β (°)	90.5977	90.5870(3)	90.590 (4)
vol (Å^3)	891.685	887.560(1)	888.238 (1)

current density of 0.2 mA cm^{-2} at room temperature. All the samples charge and discharge curves show evidence of multi-step reactions during Li extraction and insertion (Fig. 2), corresponding to two-phase reactions. During charging, the two-step extraction of the first Li (1 mol of Li) occurred at ~3.6 V ($Li_{2.5}V_2(PO_4)_3$) and ~3.7 V *vs.* Li ($Li_2V_2(PO_4)_3$) and led to the formation of a more ordered phase of $Li_2V_2(PO_4)_3$. Removal of the second Li (totally 2 mol of Li) occurred at ~4.1 V *vs.* Li with a long distinct plateau; the resulting $LiV_2(PO_4)_3$ preserved the monoclinic symmetry of the lattice [28–30]. The above three distinct plateau regions correspond to the removal of first 2 mol of Li and are associated with the V^{3+}/V^{4+} redox couple. Extraction of the final third Li (totally 3 mol of Li) occurred at ~4.55 V *vs.* Li to form de-lithiated $Li_0V_2(PO_4)_3$, comprising a mixture of valance states V^{4+} and V^{5+}. During discharging, reversible Li insertion occurred at ~3.55 V *vs.* Li; a monotonic curve followed by two distinct plateaus at ~3.6 and ~4 V *vs.* Li resulted, corresponding to the 3 mol of Li. The long monotonic curve indicates the reversible insertion of 2 mol of Li, such a curve is generally associated with the formation of a solid solution. The two short and flat discharge curves followed by a monotonic curve correspond to the re-insertion of the third Li with a bi-phase mechanism: $Li_2V_2(PO_4)_3 \rightarrow Li_{2.5}V_2(PO_4)_3 \rightarrow Li_3V_2(PO_4)_3$. Cells based on $Li_3V_2(PO_4)_3$, C-$Li_3V_{1.98}Al_{0.02}(PO_4)_3$, C-$Li_3V_{1.98}Al_{0.02}(PO_4)_{2.99}Cl_{0.01}$, C-$Li_3V_{1.98}Al_{0.02}(PO_4)_{2.97}Cl_{0.03}$ and C-$Li_3V_{1.98}Al_{0.02}(PO_4)_{2.95}Cl_{0.05}$ delivered reversible capacities of 159 (2.42 mol of Li), 172 (2.62 mol of Li), 178 (2.71 mol of Li), 176 (2.68 mol of Li) and 173 (2.63 mol of Li) mAh g^{-1}, respectively. All cases showed some irreversible capacity loss; particularly the pristine compound, due to its inherent conducting behavior and its high operating potential, which was greater than the safe operation limit of conventional carbonate-based electrolytes (>4.6 V *vs.* Li) [31]. Initial reversible capacity loss was less in the Cl^- substituted compounds than in the pristine and the C-$Li_3V_{1.98}Al_{0.02}(PO_4)_3$ materials. 0.01 mol Cl^- substitution resulted in the best cell performance. Its higher reversible capacity was attributed mainly to better kinetic properties during Li insertion and extraction, due to the Al^{3+} and Cl^- substitutions,

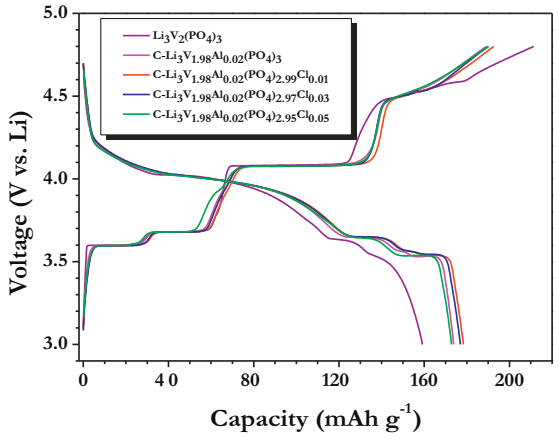

Fig. 2. Typical galvanostatic charge–discharge curves of NASICON-type materials in half-cell configurations and cycled between 3 and 4.8 V *vs.* Li at a constant current density of 0.2 mA cm^{-2} at ambient temperature.

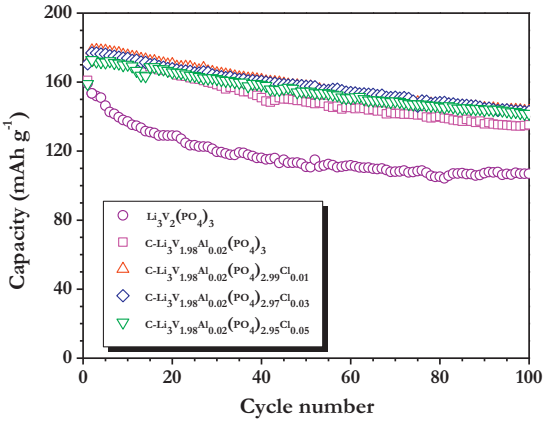

Fig. 3. Reversible capacity *vs.* cycle number for NASICON-type materials cycled between 3 and 4.8 V *vs.* Li at a constant current density of 0.2 mA cm^{-2} at ambient temperature.

which improved electronic conductivity. At higher concentration of Cl^- substitution (beyond 0.01 mol) provides the formation of Cl^- clusters over the surface results poor performance than least concentration.

Galvanostatic charge and discharge test was extended to 100 cycles under the same condition to study the samples cycling stability with respect to Cl^- concentration (Fig. 3). All the compounds showed capacity fading during cycling. This was attributed to the destruction of the crystal structure during the removal of the third mole of Li – hence most reported work has only attempted the removal of 2 mol of Li by restricting the upper cut-off potential to 4.3 V *vs.* Li. Capacity fading was believed of such phases due to the poor compatibility of vanadium compounds toward linear carbonates [32], vanadium dissolution [33] and the use of an extended potential range (upper cut-off potential 4.8 V *vs.* Li) higher than the thermodynamical stability of conventional electrolytes (~4.6 V *vs.* Li), resulting in the decomposition of the electrolyte [31]. In the second cycle, all the cathodes showed increased reversible capacity except the native compound. Capacity retentions, calculated from the second cycle onwards, were 70, 77, 80, 80 and 81% for $Li_3V_2(PO_4)_3$, C-$Li_3V_{1.98}Al_{0.02}(PO_4)_3$, C-$Li_3V_{1.98}Al_{0.02}(PO_4)_{2.99}Cl_{0.01}$, C-$Li_3V_{1.98}Al_{0.02}(PO_4)_{2.97}Cl_{0.03}$ and C-$Li_3V_{1.98}Al_{0.02}(PO_4)_{2.95}Cl_{0.05}$, respectively. This demonstrates that anion site Cl^- doping in $Li_3V_{1.98}Al_{0.02}(PO_4)_3$ provided higher reversible capacity with improved capacity retention. $(PO)_4^{3-}$ based polyanions hinder Li ions kinetics during charging and discharging, though the substitution of a small amount of Cl^- in oxygen sites was shown here to remedy the poor kinetics.

To understand the Li-ion kinetics during electrochemical charge/discharge process, a cyclic voltammetry studies (CV) were conducted and presented in Fig. 4. Only selective samples were subjected for CV analysis. It is obvious to notice the presence of very sharp intense peaks at ~3.64, ~3.72 and ~4.14 V *vs.* Li for all the three compositions tested which is associated for oxidation of V^{3+} to V^{4+} for the removal of 2 mol of Li. Another peak potential at ~4.57 V *vs.* Li corresponds to the partial oxidation of V^{4+} to V^{5+} to form de-lithiated phase. Similarly, during discharge process, oxidation peak potentials at ~4.14 and ~4.57 V *vs.* Li are merged together and appeared as broad peak at ~3.99 V *vs.* Li. This broad peak is the indication of formation of the solid-solution and associated with the reversible insertion of 2 mol of Li [30]. The less intense sharp peak potentials at ~3.61 and ~3.5 V *vs.* Li related to the insertion of 1 mol of Li. The sharp peak potentials are ascribed to the two-phase reaction mechanism and broad peak potential is due to the single phase reaction/formation of solid-solution. The observed peaks are consistent with the galvanostatic charge/discharge

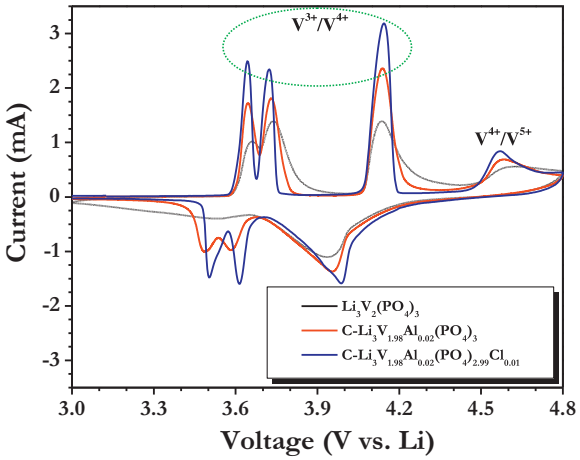

Fig. 4. Cyclic voltammetry traces of $Li_3V_2(PO_4)_3$, C-$Li_3V_{1.98}Al_{0.02}(PO_4)_3$ and C-$Li_3V_{1.98}Al_{0.02}(PO_4)_{2.99}Cl_{0.01}$ in two-electrode half-cell configurations cycled between 3 and 4.8 V *vs.* Li at slow scan rate of 0.1 mV s^{-1}. Metallic lithium was used as both counter and reference electrodes.

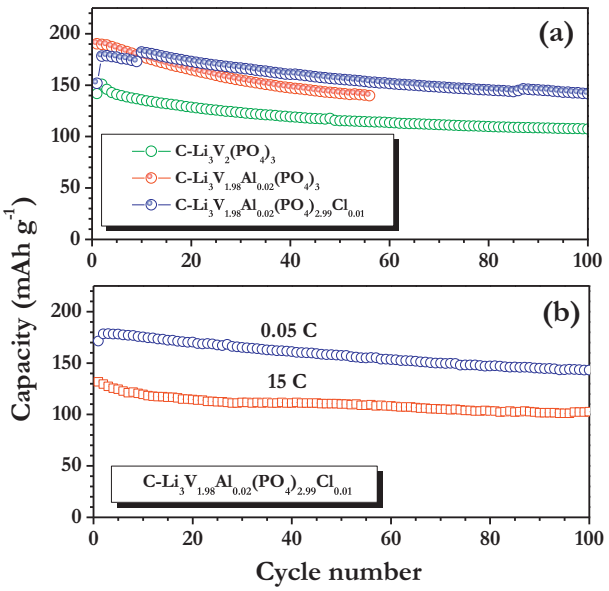

Fig. 5. (a) Galvanostatic cycling profiles of Li/C-$Li_3V_2(PO_4)_3$, Li/C-$Li_3V_{1.98}Al_{0.02}(PO_4)_3$ and Li/C-$Li_3V_{1.98}Al_{0.02}(PO_4)_{2.99}Cl_{0.01}$ cells cycled between 3 and 4.8 V *vs.* Li at a constant current density of 0.2 mA cm^{-2} at 50 °C. (b) Discharge capacity *vs.* cycle number of a Li/C-$Li_3V_{1.98}Al_{0.02}(PO_4)_{2.99}Cl_{0.01}$ cells tested between 3 and 4.8 V *vs.* Li at various current rates at ambient temperature.

curves. Variation in the peak currents are noted for $Li_3V_2(PO_4)_3$, C-$Li_3V_{1.98}Al_{0.02}(PO_4)_3$ and C-$Li_3V_{1.98}Al_{0.02}(PO_4)_{2.99}Cl_{0.01}$ cathodes, although all three test electrodes are formulated with same amount of mass loadings (20 mg). Very high peak current is noticed for C-$Li_3V_{1.98}Al_{0.02}(PO_4)_{2.99}Cl_{0.01}$ compared to rest of the two electrodes, which is mainly due to the improved Li-ion kinetics by Cl^- substitution during oxidation and reduction process. Previously, we had reported that the increase in Li-ion kinetics is enabled by vanadium site (Al^{3+}) substitution and carbon coating (C-$Li_3V_{1.98}Al_{0.02}(PO_4)_3$), which is clearly evident from the increase in peak current [9]. After the Cl^- substitution on oxygen sites drastically improves the peak current and small shifting of insertion potential toward higher voltage are observed which clearly reveal the enhanced Li-ion kinetic properties.

For high-power Li-ion cells to be used in electric vehicles, they must be able to provide high current performance at elevated temperatures [34]. Al^{3+} doped cathodes have previously shown suitability for such cells, particularly at elevated temperatures of 50 °C [9]. Half-cell configurations were assembled using $Li_3V_2(PO_4)_3$, C-$Li_3V_{1.98}Al_{0.02}(PO_4)_3$ and C-$Li_3V_{1.98}Al_{0.02}(PO_4)_{2.99}Cl_{0.01}$ and then cycled (Fig. 5(a)). Except during the initial cycles, the cell with C-$Li_3V_{1.98}Al_{0.02}(PO_4)_{2.99}Cl_{0.01}$ delivered better Li insertion characteristics than C-$Li_3V_{1.98}Al_{0.02}(PO_4)_3$ at high temperature. However, specific capacity values are increased after certain cycle which is due to the slower participation of the active material in the electrochemical reaction in such high amount of mass loading (20 mg). Here, 200 mAh g^{-1} is assumed as 1 C. Li-ion cells for electric vehicles must show high rate performances, therefore two cells were subjected for high-current testing. Reversible capacity decreased during prolonged cycling. After 100 cycles, Li/$Li_3V_{1.98}Al_{0.02}(PO_4)_{2.99}Cl_{0.01}$ half-cell delivered excellent reversible capacities of 143 and 103 mAh g^{-1} at 0.05 and 15 C rates, respectively.

To validate the influence of Cl^- substitution on the electronic conductivity profiles of NASICON type $Li_3V_2(PO_4)_3$ compounds, an electrochemical impedance spectroscopy (EIS) was recorded and presented in Fig. 6. The EIS traces contains three important parts, among them appearance of high frequency semicircle region is attributed to the solid electrolyte interface (SEI) film formation and/or contact resistance, the medium frequency region is associated with charge-transfer (CT) impedance across electrode/electrolyte interface, and 45° inclined vertical tails indicates the lithium diffusion kinetics toward the electrodes called as Warburg resistance [35]. Intercept at the Z_{real} axis in high frequency region corresponds to the ohmic resistance (R_s), which includes the total resistance of the electrolyte solution (1 M $LiPF_6$ in EC/DMC), separator and electrical contacts. The direct measurement of charge transfer (CT) impedance is mainly due to the electronic conducting properties of the any active material. It is obvious to notice that the diameter of semicircle in medium-frequency region for NASICON type materials are decreased (CT resistance) after the carbon coating and Al^{3+} doping on vanadium site. The Cl^- substitution on oxygen sites leads to the further reduction in CT resistance value which is evidently seen in Fig. 6. This EIS spectra clearly indicate that anion site doping effectively contribute to the increase in electronic conductivity of the materials and thereby improving Li-ion kinetics during electrochemical charge–discharge process. The observed increases in electronic conductivity profiles are consistent with the theoretical predictions by Dinh et al. [25].

C-$Li_3V_{1.98}Al_{0.02}(PO_4)_{2.99}Cl_{0.01}$ powder was observed by scanning electron microscopy (Fig. 7). It comprised highly aggregated, irregular particles, which emerged during solid-state reactions for

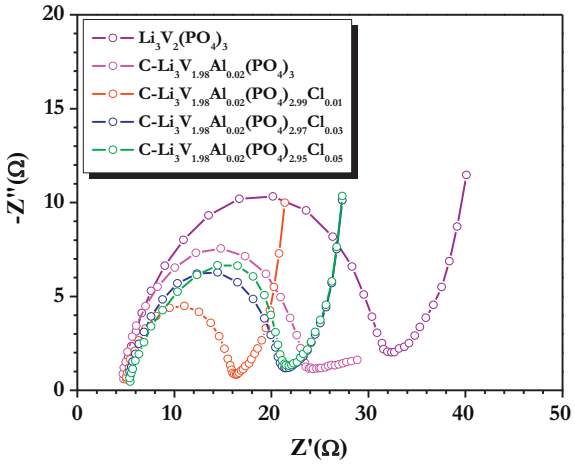

Fig. 6. Electrochemical impedance spectra (EIS) of NASICON-type powders recorded in two-electrode, coin-cell configurations.

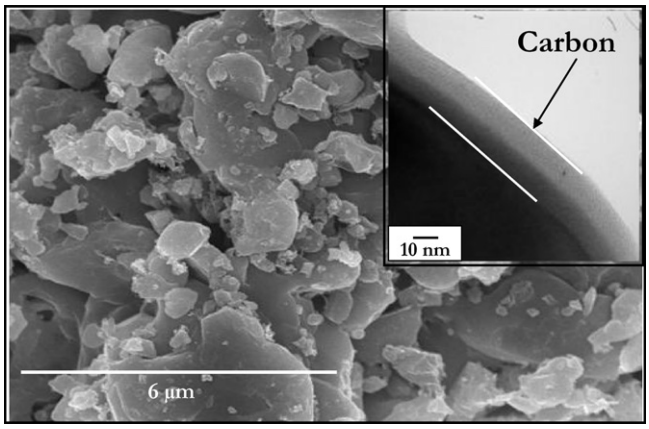

Fig. 7. Scanning electron microscopic images of C-$Li_3V_{1.98}Al_{0.02}(PO_4)_{2.99}Cl_{0.01}$ powder. Inset, high-resolution transmission electron microscopy image showing the carbon coating.

over 8 h at a relatively high temperature of 900 °C. The particles carbon coating layers, of ~10 nm thickness, were observed by high-resolution transmission election microscopy (HR-TEM, inset Fig. 7). The carbon layers were obtained *in situ* from the carbonization of adipic acid during synthesis under an inert atmosphere.

4. Conclusion

The kinetics of Li-ion insertion was enhanced in carbon-coated, NASICON-type $Li_3V_{1.98}Al_{0.02}(PO_4)_3$ materials by Cl^- substitution in oxygen sites. Phase purity and the carbon coating layer (~10 nm thickness) were confirmed through X-ray diffractometry and high-resolution transmission electron microscopy, respectively. Galvanostatic charging and discharging testing of Li insertion showed that carbon-coated $Li_3V_{1.98}Al_{0.02}(PO_4)_{2.99}Cl_{0.01}$ delivered a maximum reversible capacity of 178 mAh g^{-1} at a current density of 0.2 mA cm^{-2}. Good capacity retention over 100 cycles was observed in the Cl^- substituted materials compared with pristine and Al^{3+} doped samples. The carbon-coated $Li_3V_{1.98}Al_{0.02}(PO_4)_{2.99}Cl_{0.01}$ presented excellent cell performances under harsh conditions and elevated temperatures. These results demonstrate that Cl^- substitution in polyanionic frameworks can improve Li-ion kinetics and thereby improve battery performance. This approach could be extended to other polyanionic framework materials and could find applicability in the fabrication of high performance Li-ion power packs.

Acknowledgement

This work was supported by Energy Efficiency and Resources R&D program (20112010100150) under the Ministry of Knowledge Economy, Republic of Korea.

Appendix A. Supplementary data

Supplementary data associated with this article can be found, in the online version, at http://dx.doi.org/10.1016/j.electacta.2013.02.118.

References

[1] J. Goodenough, Rechargeable batteries: challenges old and new, Journal of Solid State Electrochemistry 16 (2012) 2019.
[2] Z. Gong, Y. Yang, Recent advances in the research of polyanion-type cathode materials for Li-ion batteries, Energy & Environmental Science 4 (2011) 3223.
[3] V. Aravindan, J. Gnanaraj, Y.S. Lee, S. Madhavi, $LiMnPO_4$– A next generation cathode material for lithium-ion batteries, Journal of Materials Chemistry A 1 (2013) 3518.
[4] N.-S. Choi, Z. Chen, S.A. Freunberger, X. Ji, Y.-K. Sun, K. Amine, G. Yushin, L.F. Nazar, J. Cho, P.G. Bruce, Challenges facing lithium batteries and electrical double-layer capacitors, Angewandte Chemie International Edition 51 (2012) 9994.
[5] P. Barpanda, S.-i. Nishimura, A. Yamada, High-voltage pyrophosphate cathodes, Advanced Energy Materials 2 (2012) 841.
[6] C.M. Hayner, X. Zhao, H.H. Kung, Materials for rechargeable lithium-ion batteries, Annual Review of Chemical and Biomolecular Engineering 3 (2012) 445.
[7] J.B. Goodenough, Y. Kim, Challenges for rechargeable Li batteries, Chemistry of Materials 22 (2009) 587.
[8] V. Aravindan, W. Chuiling, M.V. Reddy, G.V.S. Rao, B.V.R. Chowdari, S. Madhavi, Carbon coated nano-$LiTi_2(PO_4)_3$ electrodes for non-aqueous hybrid supercapacitors, Physical Chemistry Chemical Physics 14 (2012) 5808.
[9] A.R. Cho, J.N. Son, V. Aravindan, H. Kim, K.S. Kang, W.S. Yoon, W.S. Kim, Y.S. Lee, Carbon supported, Al doped-$Li_3V_2(PO_4)_3$ as a high rate cathode material for lithium-ion batteries, Journal of Materials Chemistry 22 (2012) 6556.
[10] S.M.G. Yang, V. Aravindan, W.I. Cho, D.R. Chang, H.S. Kim, Y.S. Lee, Realizing the performance of $LiCoPO_4$ cathodes by Fe substitution with off-stoichiometry, Journal of the Electrochemical Society 159 (2012) A1013.
[11] S.K. Martha, B. Markovsky, J. Grinblat, Y. Gofer, O. Haik, E. Zinigrad, D. Aurbach, T. Drezen, D. Wang, G. Deghenghi, I. Exnar, $LiMnPO_4$ as an advanced cathode material for rechargeable lithium batteries, Journal of the Electrochemical Society 156 (2009) A541.
[12] J. Barker, R.K.B. Gover, P. Burns, A. Bryan, M.Y. Saidi, J.L. Swoyer, Performance evaluation of lithium vanadium fluorophosphate in lithium metal and lithium-ion cells, Journal of the Electrochemical Society 152 (2005) A1776.
[13] Y. Makimura, L.S. Cahill, Y. Iriyama, G.R. Goward, L.F. Nazar, Layered lithium vanadium fluorophosphate, $Li_5V(PO_4)_2F_2$: a 4 V class positive electrode material for lithium-ion batteries, Chemistry of Materials 20 (2008) 4240.
[14] T.N. Ramesh, K.T. Lee, B.L. Ellis, L.F. Nazar, Tavorite lithium iron fluorophosphate cathode materials: phase transition and electrochemistry of $LiFePO_4F$-Li_2FePO_4F, Electrochemical and Solid-State Letters 13 (2010) A43.
[15] N. Recham, J.N. Chotard, J.C. Jumas, L. Laffont, M. Armand, J.M. Tarascon, Ionothermal synthesis of Li-based fluorophosphates electrodes, Chemistry of Materials 22 (2010) 1142.
[16] S. Amaresh, G.J. Kim, K. Karthikeyan, V. Aravindan, K.Y. Chung, B.W. Cho, Y.S. Lee, Synthesis and enhanced electrochemical performance of Li_2CoPO_4F cathodes under high current cycling, Physical Chemistry Chemical Physics 14 (2012) 11904.
[17] S.-W. Kim, D.-H. Seo, H. Kim, K.-Y. Park, K. Kang, A comparative study on Na_2MnPO_4F and Li_2MnPO_4F for rechargeable battery cathodes, Physical Chemistry Chemical Physics 14 (2012) 3299.
[18] B.L. Ellis, W.R.M. Makahnouk, Y. Makimura, K. Toghill, L.F. Nazar, A multifunctional 3.5 V iron-based phosphate cathode for rechargeable batteries, Nature Materials 6 (2007) 749.
[19] B. Kang, G. Ceder, Electrochemical performance of $LiMnPO_4$ synthesized with off-stoichiometry, Journal of the Electrochemical Society 157 (2010) A808.
[20] S.B. Lee, S.H. Cho, V. Aravindan, H.S. Kim, Y.S. Lee, Improved cycle performance of sulfur-doped $LiFePO_4$ material at high temperatures, Bulletin of the Korean Chemical Society 30 (2009) 2223.
[21] M. Pan, X. Lin, Z. Zhou, Electrochemical performance of $LiFePO_4$/C doped with F synthesized by carbothermal reduction method using NH_4F as dopant, Journal of Solid State Electrochemistry 16 (2012) 1615.
[22] K.-S. Park, P. Xiao, S.-Y. Kim, A. Dylla, Y.-M. Choi, G. Henkelman, K.J. Stevenson, J.B. Goodenough, Enhanced charge-transfer kinetics by anion surface modification of $LiFePO_4$, Chemistry of Materials 24 (2012) 3212.
[23] S. Zhong, L. Liu, J. Liu, J. Wang, J. Yang, High-rate characteristic of F-substitution cathode materials for Li-ion batteries, Solid State Communications 149 (2009) 1679.
[24] J. Yan, W. Yuan, Z.-Y. Tang, H. Xie, W.-F. Mao, L. Ma, Synthesis and electrochemical performance of $Li_3V_2(PO_4)_{3-x}Cl_x$/C cathode materials for lithium-ion batteries, Journal of Power Sources 209 (2012) 251.
[25] V.A. Dinh, J. Nara, T. Ohno, In vacancy formation and attractive interaction between vacancies and chlorine in chlorine-doped $LiFePO_4$, in: Nanotechnology Materials and Devices Conference (NMDC) 2011 IEEE, 2011, p. 190.
[26] C.S. Sun, Y. Zhang, X.J. Zhang, Z. Zhou, Structural and electrochemical properties of Cl-doped $LiFePO_4$/C, Journal of Power Sources 195 (2010) 3680.
[27] J.B. Goodenough, Cathode materials: a personal perspective, Journal of Power Sources 174 (2007) 996.
[28] S.C. Yin, H. Grondey, P. Strobel, M. Anne, L.F. Nazar, Electrochemical property: structure relationships in monoclinic $Li_{3-y}V_2(PO_4)_3$, Journal of the American Chemical Society 125 (2003) 10402.
[29] H. Huang, S.C. Yin, T. Kerr, N. Taylor, L.F. Nazar, Nanostructured composites: a high capacity, fast rate $Li_3V_2(PO_4)_3$/carbon cathode for rechargeable lithium batteries, Advanced Materials 14 (2002) 1525.
[30] J.N. Son, G.J. Kim, M.C. Kim, S.H. Kim, V. Aravindan, Y.G. Lee, Y.S. Lee, Carbon coated NASICON type $Li_3V_{2-x}M_x(PO_4)_3$ (M=Mn, Fe and Al) materials with enhanced cyclability for Li-ion batteries, Journal of The Electrochemical Society 160 (2013) A87.
[31] V. Aravindan, J. Gnanaraj, S. Madhavi, H.-K. Liu, Lithium-ion conducting electrolyte salts for lithium batteries, Chemistry – A European Journal 17 (2011) 14326.

[32] F. Tanguy, J. Gaubicher, P. Soudan, N. Bourgeon-Martin, V. Mauchamp, D. Guyomard, Propagation of surface-assisted side reactions, a main cause for capacity fading of vanadium oxide nanograins, Electrochemical and Solid-State Letters 10 (2007) A184.
[33] S. Patoux, C. Wurm, M. Morcrette, G. Rousse, C. Masquelier, A comparative structural and electrochemical study of monoclinic $Li_3Fe_2(PO_4)_3$ and $Li_3V_2(PO_4)_3$, Journal of Power Sources 119–121 (2003) 278.
[34] E.J. Cairns, P. Albertus, Batteries for electric and hybrid-electric vehicles, Annual Review of Chemical and Biomolecular Engineering 1 (2010) 299.
[35] V. Aravindan, K. Karthikeyan, K.S. Kang, W.S. Yoon, W.S. Kim, Y.S. Lee, Influence of carbon towards improved lithium storage properties of Li_2MnSiO_4 cathodes, Journal of Materials Chemistry 21 (2011) 2470.